

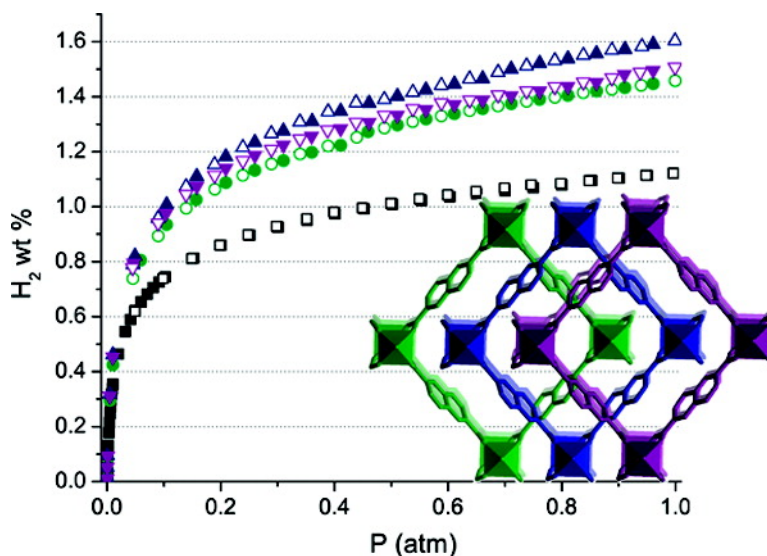
Article

Framework Reduction and Alkali-Metal Doping of a Triply Catenating Metal#Organic Framework Enhances and Then Diminishes H Uptake

Karen L. Mulfort, Thea M. Wilson, Michael R. Wasielewski, and Joseph T. Hupp

Langmuir, 2009, 25 (1), 503-508 • DOI: 10.1021/la803014k • Publication Date (Web): 10 December 2008

Downloaded from <http://pubs.acs.org> on February 11, 2009



More About This Article

Additional resources and features associated with this article are available within the HTML version:

- Supporting Information
- Access to high resolution figures
- Links to articles and content related to this article
- Copyright permission to reproduce figures and/or text from this article

[View the Full Text HTML](#)



ACS Publications
High quality. High impact.

Langmuir is published by the American Chemical Society, 1155 Sixteenth Street N.W., Washington, DC 20036

Framework Reduction and Alkali-Metal Doping of a Triply Catenating Metal–Organic Framework Enhances and Then Diminishes H₂ Uptake

Karen L. Mulfort,^{†,‡} Thea M. Wilson,[†] Michael R. Wasielewski,[†] and Joseph T. Hupp^{*,†}

Department of Chemistry & Argonne-Northwestern Solar Energy Research (ANSER) Center, Northwestern University, 2145 Sheridan Road, Evanston, Illinois 60208, and Division of Chemical Sciences and Engineering, Argonne National Laboratory, 9700 South Cass Avenue, Argonne, Illinois 60439

Received September 14, 2008

A permanently microporous metal–organic framework compound with the formula Zn₂(NDC)₂(diPyTz) (NDC = 2,6-naphthalenedicarboxylate, diPyTz = di-3,6-(4-pyridyl)-1,2,4,5-tetrazine) has been synthesized. The compound, which features a triply catenating, pillared-paddlewheel structure, was designed to be easily chemically reduced (diPyTz sites) by appropriate channel permeants. Reduction was achieved by using the naphthalenide anion, with the accompanying metal cation (Li⁺, Na⁺ or K⁺) serving to dope the compound in extraframework fashion. H₂ uptake at 1 atm and 77 K increases from 1.12 wt % for the neutral material to 1.45, 1.60, and 1.51 wt % for the Li⁺-, Na⁺-, and K⁺-doped materials, respectively. The isosteric heats of adsorption are similar for all four versions of the material despite the large uptake enhancements for the reduced versions. Nitrogen isotherms were also measured in order to provide insight into the mechanisms of uptake enhancement. The primary mechanism is believed to be dopant-facilitated displacement of catenated frameworks by sorbed H₂. More extensive cation doping decreases the H₂ loading.

1. Introduction

Permanently microporous, crystalline, metal–organic framework materials (MOFs) are being considered for a wide range of chemical applications that can capitalize on their high internal surface areas, uniform pore sizes, and enormous potential diversity in composition and structure.^{1–3} Among the most intriguing is hydrogen gas storage.^{4–6} MOFs have the capacity to revolutionize gas storage methods and materials because of their ultralow densities and their crystalline micropore and/or ultramicropore structures; in principle, these structures can promote ordered and therefore exceptionally high density guest packing. There have been several recent reports of large H₂ uptake in MOFs at 77 K and high pressure,^{7,8} but none yet satisfy the proposed capacity benchmarks for commercially viable and safe hydrogen storage at noncryogenic temperatures. Although there is an immediate need to improve H₂ sorption, equally important for long-term success is the need to understand fully the factors that affect H₂ uptake and binding such that the essentially limitless potential variety of MOF materials can be used to full advantage.

Improving MOF H₂ adsorption capacity through structural means has been pursued by two general strategies. The first is to manipulate the MOF structure to increase H₂–framework dispersion interactions and decrease unused pore space, either

by adjusting ligand the length and shape^{9,10} or through framework catenation.¹¹ Because H₂ contains only two electrons, these dispersion interactions are relatively weak. Furthermore, they decrease with 1/*r*⁶ where *r* is the distance between H₂ and the framework. Under the storage temperatures and pressures envisioned for vehicular applications, H₂ is well above its critical point. Significant sorption excesses, therefore, can be achieved only by framework adsorption, not by pore condensation. Thus, there is no incentive to create huge pores (i.e., pores that can accommodate more than a monolayer of H₂ molecules). The second approach attempts to create exceptionally attractive surface sites within the MOF via the formation of unsaturated metal centers typically through the removal of coordinated solvent molecules at nodes (metal ions or clusters comprising framework structural sites).^{12–15} Neutron-scattering experiments have verified that H₂ binds at these sites first, most likely through Kubas-type interactions. Whereas this approach has been shown to impact H₂ uptake within MOFs appreciably, it is sometimes difficult to synthesize frameworks that can resist collapse upon complete desolvation of metal sites. A further challenge is to introduce enough such sites to make a practical difference under high-loading conditions.

We recently communicated preliminary results for a distinct but related third approach: chemical reduction of framework struts. For a representative doubly interpenetrating MOF, we observed a 75% increase in H₂ uptake at 77 K and 1 atm

* Author to whom correspondence should be addressed. E-mail: j-hupp@northwestern.edu.

[†] Northwestern University.

[‡] Argonne National Laboratory.

(1) James, S. L. *Chem. Soc. Rev.* **2003**, 32, 276–288.

(2) Kitagawa, S.; Kitaura, R.; Noro, S. *Angew. Chem., Int. Ed.* **2004**, 43, 2334–2375.

(3) Rowsell, J. L. C.; Yaghi, O. M. *Microporous Mesoporous Mater.* **2004**, 73, 3–14.

(4) Collins, D. J.; Zhou, H.-C. *J. Mater. Chem.* **2007**, 17, 3154–3160.

(5) Latroche, M.; Surble, S.; Serre, C.; Mellot-Draznieks, C.; Llewellyn, P. L.; Lee, J. H.; Chang, J. S.; Jung, S. H.; Férey, G. *Angew. Chem., Int. Ed.* **2006**, 45, 8227–8231.

(6) Lin, X.; Jia, J.; Hubberstey, P.; Schroder, M.; Champness, N. R. *CrystEngComm* **2007**, 9, 438–448.

(7) Furukawa, H.; Miller, M. A.; Yaghi, O. M. *J. Mater. Chem.* **2007**, 17, 3197–3204.

(8) Dinca, M.; Dailly, A.; Liu, Y.; Brown, C. M.; Neumann, D. A.; Long, J. R. *J. Am. Chem. Soc.* **2006**, 128, 16876–16883.

(9) Lin, X.; Jia, J.; Zhao, X.; Thomas, K. M.; Blake, A. J.; Walker, G. S.; Champness, N. R.; Hubberstey, P.; Schroeder, M. *Angew. Chem., Int. Ed.* **2006**, 45, 7358–7364.

(10) Dybtsev, D. N.; Chun, H.; Yoon, S. H.; Kim, D.; Kim, K. *J. Am. Chem. Soc.* **2004**, 126, 32–33.

(11) Ma, S. Q.; Sun, D. F.; Ambrogio, M.; Fillinger, J. A.; Parkin, S.; Zhou, H. C. *J. Am. Chem. Soc.* **2007**, 129, 1858–1859.

(12) Dinca, M.; Han, W. S.; Liu, Y.; Dailly, A.; Brown, C. M.; Long, J. R. *Angew. Chem., Int. Ed.* **2007**, 46, 1419–1422.

(13) Forster, P. M.; Eckert, J.; Heiken, B. D.; Parise, J. B.; Yoon, J. W.; Jung, S. H.; Chang, J. S.; Cheetham, A. K. *J. Am. Chem. Soc.* **2006**, 128, 16846–16850.

(14) Georgiev, P. A.; Albinati, A.; Mojet, B. L.; Ollivier, J.; Eckert, J. *J. Am. Chem. Soc.* **2007**, 129, 8086–8087.

(15) Farha, O. K.; Spokoyney, A. M.; Mulfort, K. L.; Hawthorne, M. F.; Mirkin, C. A.; Hupp, J. T. *J. Am. Chem. Soc.* **2007**, 129, 12680–12681.

(0.93→1.63 wt %) as well as significant increases in loading-dependent heats of adsorption, following partial reduction with lithium metal.¹⁶ We suggested that framework reduction could potentially enhance the uptake of H₂ by MOFs by at least three mechanisms: (i) greatly enhanced strut polarizability, potentially resulting in stronger induced-dipole/induced-dipole interactions between the strut and H₂ (i.e., $1/r^6$ interactions); (ii) the introduction of essentially completely unsaturated metal centers in the form of charge-compensating cations (potential sites for charge/quadrupole interactions with dihydrogen or Kubas interactions if transition-metal ions are used); and (iii) the displacement of interwoven networks to create pores and channels of more optimal size for H₂ sorption. On the basis of several lines of evidence, including an unusual and highly hysteretic N₂ isotherm, we concluded that (at least) mechanism iii was important for the particular system examined. We were unable to draw conclusions about the significance of mechanism ii, in part because of ambiguity in the degree of residual solvation of the dopant metal ions and in part because only a single dopant (Li⁺) was examined. In a follow-up study pursued in parallel with the present study,¹⁷ we concluded that mechanism ii was likely not operative for the doubly interpenetrating system. The follow-up work entailed an extension of the investigation of Na⁺ and K⁺ as dopants.

In this article, we report further on the idea of the chemical reduction of organic struts as a strategy for enhancing H₂ uptake by metal–organic framework compounds. As in the initial report, we employ a mixed-strut material featuring a pillared-paddlewheel structure. MOFs of this kind consist of metal pairs (generally Zn(II) or Cu(II)) bridged by linear dicarboxylates that create paddlewheel sheets in two dimensions. The sheets are pillared in a third direction by linear dipyridyls to give the overall formula M₂(dicarboxylate)₂(dipyridyl).¹⁸ We have found the motif particularly useful for creating anisotropic channel structures and for introducing catalytic¹⁹ and/or redox-active ligands. Furthermore, in contrast to many MOF materials based solely on dipyridyl struts, pillared paddlewheels typically retain their crystallinity and microporosity upon removal of the solvent.

In our experience, most pillared-paddlewheel materials, including the MOF previously subjected to framework reduction, are composed of doubly interwoven structures. Here we report the behavior of the solvent-evacuated form of triply interwoven compound Zn₂(NDC)₂(diPyTz)·nDMF (1·nDMF) (NDC = 2,6-naphthalenedicarboxylate, diPyTz = di-3,6-(4-pyridyl)-1,2,4,5-tetrazine) (Figure 1). We have subjected the material to reduction and doping with three alkali metal cations: Li⁺, Na⁺, and K⁺. We again reasoned that charge/quadrupole interactions, for example, could be systematically modulated because they depend on ion size. We find that reduction and doping, even at low levels, increase the low pressure (1 atm), cryogenic (77 K) uptake of H₂ by (solvent-evacuated) 1 by as much as 43%.

2. Experimental Methods

2.1. General Methods. All commercial reagents were of ACS grade and were purchased from Sigma-Aldrich unless otherwise noted. Tetrahydrofuran (THF) was purified using a two-column solid-state purification system (Glasscontour System, Jeorg Meyer, Irvine, CA). The synthesis of diPyTz has been previously reported.²⁰ Elemental analyses were performed by Atlantic Microlabs, Inc.

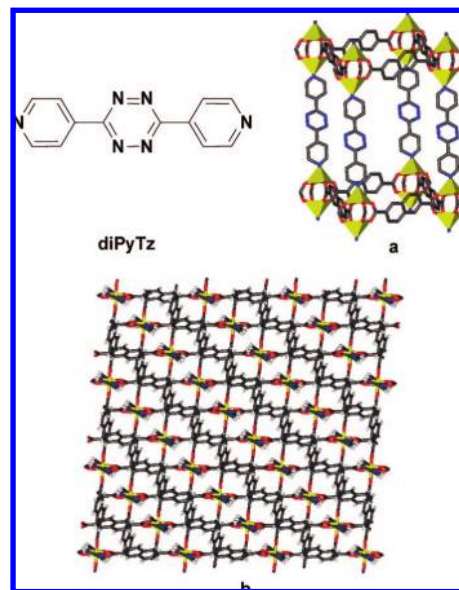


Figure 1. Chemical structure of dipyridyl ligand diPyTz, structure of 1. (A) Single-crystal structure of 1. For clarity, two levels of interpenetration are omitted. The yellow polyhedra represent the zinc ions; gray, carbon; blue, nitrogen; and red, oxygen. Hydrogens are omitted for clarity. (B) Packing diagram of 1.

(Norcross, GA). Powder X-ray diffraction (PXRD) patterns were recorded with a Rigaku XDS 2000 diffractometer using nickel-filtered Cu K α radiation ($\lambda = 1.5418$ Å) over a range of $5^\circ < 2\theta < 40^\circ$ in 0.1° steps with a 1 s counting time per step. Powder samples were placed in the diffractometer mounted on a stainless steel holder with double-sided tape. Thermogravimetric analyses (TGA) were performed on a Mettler-Toledo TGA/SDTA851e. Samples (3–5 mg) in alumina pans were heated from 25 to 700 °C at 10 °C/min under N₂. Inductively coupled plasma (ICP) spectroscopy was conducted on a Varian model ICP spectrometer that is equipped to cover the spectral range from 175 to 785 nm. Samples (3–5 mg) were digested in 1:1 H₂SO₄/H₂O₂ and heated to 120 °C until the solution became clear and colorless and no further vapor was produced. An aliquot of this concentrated acid solution was diluted to 5% with DI H₂O and analyzed for M (Li at 610.365 nm, Na at 589.592 nm, or K at 766.491 nm) and Zn (202.548 nm) content as compared to that in standardized solutions. ¹H NMR (500 MHz) measurements were performed on 1·M samples after adsorption measurements (complete evacuation) and following sample dissolution in D₂SO₄ (96–98 wt % in D₂O, 99.5 atom % D).

2.2. Synthesis of Zn₂(NDC)₂(diPyTz)·nDMF (1·nDMF). Single crystals of 1 were obtained by heating Zn(NO₃)₂·6H₂O (14 mg, 0.05 mmol), H₂NDC (10 mg, 0.05 mmol), and diPyTz (6 mg, 0.025 mmol) in 5 mL of *N,N'*-dimethylformamide (DMF) to 100 °C and heated in a sealed vial for 2 days. Then the mother liquor was decanted from the crystals, and the remaining solid was washed with DMF, and dried in air. Anal. Calcd for evacuated 1·1H₂O, C₃₆H₂₀N₆O₉Zn₂: C, 53.16; H, 2.73; N, 10.33. (Note that a much more rigorous protocol for framework evacuation and for preventing the readsorption of atmospheric water was employed in the sorption studies described below.) Found: C, 53.05; H, 2.61; N, 10.27. Structure and purity are further supported by PXRD and TGA (Supporting Information).

2.3. X-ray Crystallography. Single crystals were mounted on a Bruker Smart CCD 1000 diffractometer equipped with a graphite-monochromated Mo K α ($\lambda = 0.71073$ Å) radiation source in a cold nitrogen stream. All crystallographic data were corrected for Lorentz

(16) Mulfort, K. L.; Hupp, J. T. *J. Am. Chem. Soc.* **2007**, *129*, 9604–9605.

(17) Mulfort, K. L.; Hupp, J. T. *Inorg. Chem.* **2008**, *47*, 7936–7938.

(18) Ma, B. Q.; Mulfort, K. L.; Hupp, J. T. *Inorg. Chem.* **2005**, *44*, 4912–4914.

(19) Cho, S.-H.; Ma, B.; Nguyen, S. T.; Hupp, J. T.; Albrecht-Schmitt, T. E. *Chem. Commun.* **2006**, 2563–2565.

(20) Dinolfo, P. H.; Williams, M. E.; Stern, C. L.; Hupp, J. T. *J. Am. Chem. Soc.* **2004**, *126*, 12989–13001.

and polarization effects (SAINT) and face-index absorption corrections. The structures were solved by direct methods and refined by the full-matrix least-squares method on F^2 with appropriate software implemented in the SHELXTL program package. Most of the non-hydrogen atoms were refined anisotropically. Several of the atoms in the diPyTz ligand were refined isotropically as a result of poor data. Additionally, there was a large amount of residual electron density surrounding the diPyTz ligand in the structure, which is again a result of poor data quality. Hydrogen atoms were added at their geometrically ideal positions. Most of the DMF solvent molecules are severely disordered, which hindered satisfactory development of the model; therefore, the SQUEEZE routine (PLATON)²¹ was applied to remove the contributions of electron density from disordered solvent molecules. The outputs from the SQUEEZE calculations are attached to the cif file. Attempts were made to grow additional single crystals to obtain better-quality data, but none were successful. CCDC 672283 contains the supplementary crystallographic data for this paper. These data can be obtained free of charge from The Cambridge Crystallographic Data Centre via www.ccdc.cam.ac.uk/data_request.cif.

2.4. Framework Reduction. Reductant solutions of the three metal naphthalenides (M(NAP)) were prepared by adding an equimolar amount of an alkali metal (Li⁰, Na⁰, K⁰) to a 0.1 M solution of naphthalene in tetrahydrofuran (THF) following literature precedent.²² **Caution!** *Alkali metals are extremely reactive with water and potentially reactive with nitrogen.* All manipulations with alkali metals were carried out in an argon-atmosphere glovebox. Alkali metals are stored in mineral oil in a glovebox. All reduced materials were prepared in the same manner; a general procedure follows. Immediately prior to use, small pieces of the metal are briefly immersed in THF to remove excess mineral oil. The pieces are dried, and any dark oxide on the surface is removed to reveal the shiny metallic surface. Upon addition of the cleaned metal pieces to the naphthalene solution, a green color appears in solution. After several hours, the metal chunks are completely dissolved, and the solution is uniformly dark green. A precise quantity of 0.1 M M(NAP) is then transferred to a known amount of an MOF sample with a volumetric syringe and stirred for several minutes. The solution immediately turns clear and colorless and is accompanied by a color change in the solid. The solid MOF is then isolated on a coarse glass frit and washed with 1 mL aliquots of THF to remove any weakly adsorbed naphthalene. Versions of structure **1** reduced with M(NAP) are designated **1**·M where M = Li, Na, or K. These reduced MOFs are air-sensitive, and oxidation can be observed as the solid changes back to the original color upon exposure to air. Therefore, all manipulations with the reduced material are carried out under an inert atmosphere. The metal content is determined by ICP analysis and EA. The structure of **1** is maintained through reduction and oxidation in air as verified by PXRD and TGA (Supporting Information). Zn₂(NDC)₂(diPyTz)·Li_{0.10} (**1**·Li): Anal. Calcd. for **1**·Li, C₃₆H₂₂N₆O₉Zn₂Li_{0.10}: C, 53.11; H, 2.72; N, 10.32. Found: C, 53.38; H, 2.64; N, 10.06. Zn₂(NDC)₂(diPyTz)·Na_{0.24} (**1**·Na): Anal. Calcd. for **1**·Na, C₃₆H₂₄N₆O₁₀Zn₂Na_{0.24}: C, 51.66; H, 2.89; N, 10.04. Found: C, 51.84; H, 2.63; N, 9.79. Zn₂(NDC)₂(diPyTz)·K_{0.14} (**1**·K): Anal. Calcd. for **1**·K, C₃₆H₂₄N₆O₁₀Zn₂K_{0.14}: C, 51.67; H, 2.89; N, 10.26. Found: C, 50.39; H, 2.34; N, 9.55.

2.5. Adsorption Measurements. Low-pressure nitrogen and hydrogen adsorption measurements were carried out on an Autosorb 1-MP from Quantachrome Instruments. Ultrahigh purity He, H₂, and N₂ were used for adsorption measurements. Prior to analysis, materials were loaded into a sample tube of known weight and heated to 110 °C under dynamic vacuum for ~24 h to remove guest solvent and fully activate samples. Samples of **1**·M are air- (oxygen-) sensitive and were loaded into sample tubes under an inert atmosphere (argon). Additionally, because of the oxygen sensitivity of **1**·M materials and the potential for sorption of water from the air, the sample tubes were backfilled with an inert atmosphere (He or N₂) before transfer between the activation and analysis ports. After evacuation and analysis, the sample and tube were reweighed to

Table 1. Crystallographic Data for **1**·nDMF

1 ·nDMF	
empirical formula ^a	C ₃₆ H ₂₀ N ₆ O ₈ Zn ₂
formula weight	795.36
crystal color, habit	pink, block
crystal dimensions, mm ³	0.057 × 0.050 × 0.028
crystal system	triclinic
space group	$P\bar{1}$
<i>a</i> (Å)	7.8153(23)
<i>b</i> (Å)	10.7462(32)
<i>c</i> (Å)	13.0279(45)
α (deg)	70.845(7)
β (deg)	72.778(4)
γ (deg)	88.703(5)
<i>V</i> (Å ³)	983.85
<i>Z</i>	2
<i>T</i> (K)	77
ρ (calcd, g/cm ³)	1.339
μ (cm ⁻¹)	1.27
goodness-of-fit on F^2	1.112
R^b	0.1351
R_w^c	0.3686

^a The SQUEEZE routine in PLATON was employed to mask diffuse electron density in the cavities due to disordered solvent (DMF) molecules.

^b $R(F) = (\Sigma F_o - F_c)/\Sigma F_o$. ^c $R_w(F_o^2) = [\Sigma w(F_o^2 - F_c^2)^2/\Sigma wF_o^4]^{1/2}$.

obtain the precise mass of the evacuated sample. N₂ adsorption isotherms were measured at 77 K; H₂ adsorption isotherms were measured at both 77 and 87 K in order to obtain isosteric heats of adsorption.

2.6. EPR Measurements. Samples were prepared in an argon atmosphere glovebox by loading the crystalline powder into quartz capillary tubes (0.84 mm o.d., 0.6 mm i.d.) that were then inserted into larger quartz tubes for easier handling and sealing. The tubes were sealed with a plug of vacuum grease and wrapped tightly with parafilm. Continuous wave (CW) EPR measurements were made using a Bruker Eleksys E580 X-band EPR spectrometer outfitted with a variable-*Q* dielectric resonator (ER-4118X-MD5-W1). All measurements were made at room temperature (~295 K) at a microwave power of 2 mW and a frequency modulation depth of 100 kHz.

3. Results and Discussion

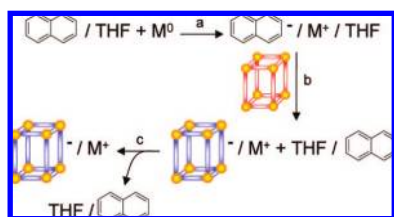
3.1. Structure of **1·nDMF.** Macroscopic crystals of **1**·nDMF, obtained from static heating of the individual components in DMF (Experimental Section), were structurally characterized by single-crystal X-ray diffraction (Table 1). The connectivity of one network of **1** is shown in Figure 1a. Like other paddlewheel MOFs, it exhibits pillared square-grid network topology. The structure features 3-fold catenation (Figure 1b) but still has a 27% solvent-accessible void volume.²³

3.2. Framework Reduction. Ligand diPyTz was chosen as a framework strut because of its well-defined redox activity.²⁰ In related discrete coordination compounds, the ligand exhibits reversible one-electron reductions at −1.81 and −2.50 V versus ferrocene⁺⁰. Framework-permeating metal naphthalenide species (M(NAP)) were employed for doping and reduction. M(NAP) species are powerful reductants ($E^\circ = -3.10$ V vs Fc/Fc⁺ in THF) but otherwise are chemically inert.²² The naphthalenide-anion-containing solution is intensely green. When added to the solid MOF, the solution turns clear/colorless as the naphthalenide radical anion transfers an electron to the dipyrilidyl ligand within the MOF (Scheme 1 and Figure 2). The resulting cation-doped MOF (designated **1**·M, where M is Li⁺, Na⁺, or K⁺) is easily separated from the reductant solution via filtration. PXRD revealed that the framework retains crystallinity upon reduction (Sup-

(21) Spek, A. L. *J. Appl. Crystallogr.* **2003**, *36*, 7–13.

(22) Connelly, N. G.; Geiger, W. E. *Chem. Rev.* **1996**, *96*, 877–910.

(23) Xue, M.; Ma, S.; Jin, Z.; Schaffino, R. M.; Zhu, G.-S.; Lobkovsky, E. B.; Qiu, S.-L.; Chen, B. *Inorg. Chem.* **2008**, *47*, 6825–6828.

Scheme 1. Chemical Reduction of MOF Using Metal Naphthalenide (M(NAP)) in THF^a


^a (a) Addition of metal to naphthalene in THF, (b) introduction of M(NAP)-THF solution into solid MOF, (c) isolated reduced MOF by filtration. In this study, M is Li, Na, or K.

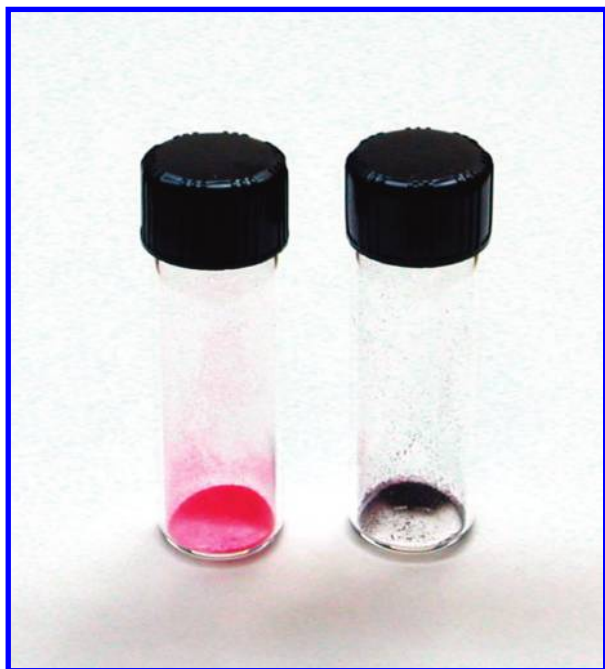


Figure 2. Visual observation of framework reduction. Picture of color change in **1** (left, pink) upon exposure to lithium naphthalenide to form **1·Li** (right, dark purple) (Li/diPyTz = 0.56).

Table 2. Summary of N₂ and H₂ Adsorption Measurements of **1 and **1·M****

	M/Zn ^a	M/diPyTz	surface area (m ² /g) ^b	micropore volume (cm ³ /g) ^c	H ₂ wt % (1 atm, 77 K)	Q _{st} range (kJ/mol)
1	0.00	0.00	400/314	0.16	1.12	8.5–6.5
1·Li	0.05	0.10	526/365	0.19	1.46	8.3–6.1
1·Na	0.12	0.24	558/419	0.21	1.60	8.7–4.0
1·K	0.07	0.14	509/378	0.20	1.51	8.9–4.4
1·Li*	0.35	0.70	163/134	0.07	0.54	9.0–5.0

^a Determined by ICP analysis. ^b The first value in each column is calculated by BET analysis of the N₂ isotherm at 0.05 < P/P₀ < 0.30; the second value is obtained from a t-plot analysis of the N₂ isotherm and includes only the surface area attributable to micropores. ^c Calculated from the t-plot analysis of N₂ adsorption.

porting Information). Whereas small changes to the PXRD pattern are evident following reduction and doping, we are unable to translate these into specific structural changes.

The degree of reduction and concurrent metal loading are controlled by the amount of reductant solution added to the solid MOF. We find that improved adsorption performance for these materials is obtained at doping levels that are much lower than 1 cation per dipyrindyl ligand; the greatest enhancements are found for M/Zn ≈ 0.05 to 0.10 (Table 2). Further doping (which was not explored in detail) leads to less effective H₂ uptake. (For

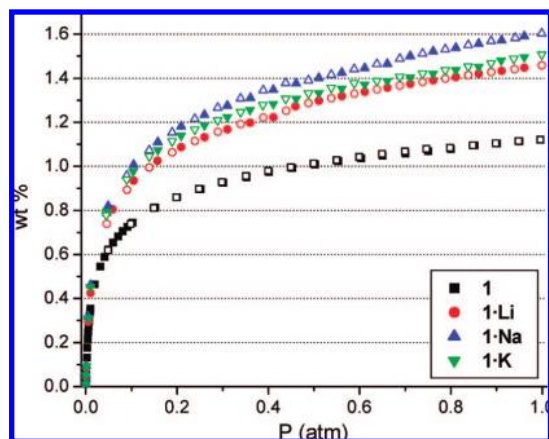


Figure 3. H₂ adsorption isotherms at 77 K of **1** and **1·M**. Closed symbols, adsorption; open symbols, desorption.

example, increasing Li/Zn from 0.05 to 0.35 caused the H₂ loading at 77 K and 1 atm to *drop* by ca. (relatively) 50%; see Table 2 and Supporting Information.) This finding, although unusual, is consistent with our earlier observations for a doubly catenating compound.^{16,17} The dipyrindyl strut of **1** is thermodynamically much easier to reduce than the dicarboxylate strut (NDC). Because substoichiometric amounts of reductant are used, we assume that only the diPyTz strut is reduced. Solid-state room-temperature CW-EPR measurements on **1·Li** indicated the presence of radical species within the framework, but the fine structure could not be resolved sufficiently to characterize further the nature of the reduction site (Supporting Information). There have been three recent reports on cation(metal) exchange within MOF materials and the roles that various metal centers play in H₂ uptake and binding,^{24–26} but as far as we are aware, experimental studies of ligand-centered redox behavior/doping within an MOF material are limited to the current investigation and our recent studies of a doubly interwoven system.^{16,17}

3.3. Gas Uptake and Binding. Low-pressure H₂ and N₂ isotherms were measured for **1** and all **1·M** to examine the effects that framework reduction and alkali metal doping have on H₂ uptake and on structural characteristics of the frameworks. As shown in Figure 3, H₂ uptake by the three reduced materials, **1·M**, considerably exceeds that for the neutral MOF. Interestingly, the greatest gravimetric uptake is observed with **1·Na**, despite the greater contribution of Na⁺ (in comparison to that of Li⁺) to the overall mass of the framework. Attempts to enhance uptake even further by increasing the doping level (see, for example, **1·Li*** in Table 2 and Supporting Information) actually resulted in diminished H₂ uptake in comparison to that of the original material.

To gain some insight into the differences in affinity for hydrogen, isosteric heats of adsorption, Q_{st}, were determined. The isosteric heat is a measure of the strength of H₂ interaction with the host material (i.e., framework, dopant, or both).^{27,28} Values were obtained by fitting a virial-type equation to the 77 and 87 K H₂ adsorption isotherms.²⁹ Figure 4 and Table 2 summarize the results. In all four cases, Q_{st} decreases with increasing loading. Behavior of this kind is generally indicative of adsorption-site heterogeneity. The sites with the highest binding

(24) Dinca, M.; Long, J. R. *J. Am. Chem. Soc.* **2007**, *129*, 11172–11176.

(25) Kaye, S. S.; Long, J. R. *J. Am. Chem. Soc.* **2005**, *127*, 6506–6507.

(26) Kaye, S. S.; Long, J. R. *Chem. Commun.* **2007**, 4486–4488.

(27) Lochan, R. C.; Head-Gordon, M. *Phys. Chem. Chem. Phys.* **2006**, *8*, 1357–1370.

(28) Bhatia, S. K.; Myers, A. L. *Langmuir* **2006**, *22*, 1688–1700.

(29) Czepirski, L.; Jagiello, J. *Chem. Eng. Sci.* **1989**, *44*, 797–801.

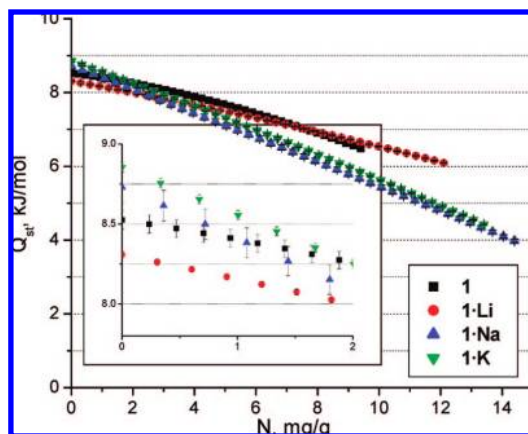


Figure 4. Isothermic H₂ heat of adsorption of **1** and **1**·**M**. Details of the behavior at low loading is depicted in the inset.

energy are filled first, and as the pressure is increased, incoming molecules fill other surface sites. There is a general consensus that the most favorable binding sites for H₂ in conventional MOFs are metal corners^{30,31} and several groups have been successful in creating unsaturated metal centers at the corners to engender extremely favorable H₂ binding within these materials.⁸

It is tempting to ascribe the behavior encountered here, especially at low hydrogen loading, to the preferential interaction of H₂ with dopant metals and/or highly polarizable reduced struts. By chemically reducing the frameworks, we are effectively introducing additional metal centers interspersed throughout the material. Furthermore, the added metal ions should be essentially *completely* coordinatively unsaturated, which should engender very high initial heats of adsorption. A comparison of Q_{st} values for doped and undoped versions of the MOF, however, does not provide support for the notion of strong adsorption at dopant metal sites. Although minor differences can be seen, the more striking observation (Figure 4) is just how closely isosteric heats agree for **1**, **1**·**Li**, **1**·**Na**, and **1**·**K** over the entire range of H₂ pressures examined.

We conclude from the above that direct hydrogen/dopant-cation interactions are *not* responsible for the enhanced H₂ uptake illustrated in Figure 3. Because this stands in contrast to our initial expectations as well as expectations from recent computational studies of reduced MOFs^{32–36} and earlier computational studies of carbon-based materials,^{37–39} we infer that the added metal ions are simply inaccessible to hydrogen. Two scenarios can be envisioned: (1) dopant cations localized near negatively charged carboxylates which effectively shielded them from gas exposure on account of framework interpenetration or (2) dopant cations strongly solvated (by DMF or THF molecules).

To test the second idea, we determined the post evacuation solvent content of the **1**·**M** materials via ¹H NMR. Samples were dissolved in 97% D₂SO₄(aq), and ratios of solvent molecules to

Table 3. Summary of ¹H NMR Quantification of Solvent Content in **1** and **1**·**M**^a

	M/Zn (II) dimer	DMF/Zn(II) dimer ^b	mass loss (%)	DMF/M ^{+c}
1 · <i>n</i> DMF	0.00	1.43	13.1	n/a
1	0.00	0.18	1.6	n/a
1 · Li	0.10	0.18	1.7	1.8
1 · Na	0.24	0.07	0.6	0.28
1 · K	0.14	0.04	0.3	0.26
1 · Li '	0.18	0.16	1.5	0.89
1 · Li ''	0.23	0.15	1.4	0.67

^a See Supporting Information for ¹H NMR and integration. ^b 20H/Zn(II) dimer calculated from the crystal structure of **1**. ^c M loading content in Table 1.

struts were calculated by integrating the respective peak intensities. As a starting point, as-synthesized (nonevacuated) **1**·*n*DMF was dissolved in D₂SO₄, and the DMF proton peaks were compared with the peaks from the framework components. The NMR-measured solvent content of **1**·*n*DMF was found to be in reasonably good agreement with that from the crystal structure: 1.4 DMF per Zn(II) dimer by NMR and 1.9 DMF per Zn(II) dimer by crystallography (Supporting Information). As shown in Table 3, the DMF content of **1**·**Na** and **1**·**K** is very low and is probably best interpreted as incomplete framework evacuation rather than residual cation solvation. (At most, the data are consistent with the solvation of one in four dopant ions by a single DMF molecule.) For **1**·**Li**, however, the significance of the initially obtained results (~1.8 DMF/Li⁺) was less clear. Consequently, the experiments were repeated with more heavily doped samples (**1**·**Li**' and **1**·**Li**''). As shown in Table 3, the residual solvent content is independent of lithium cation loading, indicating that not-quite-complete framework evacuation rather than the solvation of dopant ions accounts for the small amount of solvent found. We can therefore rule out cation solvation as a factor in the adsorption performance (e.g., surprisingly small Q_{st} values) of the reduced materials.

Separate measurements revealed that no detectable naphthalene (from M(NAP); see Scheme 1) is retained in framework-reduced materials. The proton peaks for naphthalene are sufficiently upfield from those of NDC to permit easy observation. The solubility of any potentially remaining naphthalene was ensured by dissolving the frameworks in 1:9 DMF/D₂SO₄ rather than D₂SO₄ alone.

Quantitative comparisons at 1 atm and 77 K show that low-level doping with Li⁺, Na⁺, and K⁺ increases H₂ uptake by 13, 8, and 11 molecules per alkali metal ion, respectively. (Interestingly, these numbers are greater than the maximum number of hydrogen molecules capable of directly interacting even with completely free cations.) The experiments above allow us to rule out both direct interactions with dopant ions and enhanced interactions with reduced struts as causes of the enhanced uptake. A third possible explanation is the displacement of interwoven frameworks, by dopant ions, such that the internal surface area increases. Compelling evidence for such behavior was found in our studies of hydrogen uptake by a doubly interwoven material.^{16,17}

Microporous surface areas are in principle obtainable via analysis of N₂ isotherms. An inspection of the low-temperature (77 K) isotherms in Figure 5 reveals (a) very strong adsorption by all four materials, (b) type I curve shapes (indicating microporosity), and (c) significantly greater uptake of nitrogen by the various **1**·**M** species relative to that of undoped **1** in the type I region (plateau region). Although it is tempting to interpret the differences in the plateau region in terms of differences in surface area, such a conclusion is not justified for a microporous material as its value in the plateau region is largely governed by pore filling, which is only indirectly related to surface area.

(30) Rosi, N. L.; Eckert, J.; Eddaoudi, M.; Vodak, D. T.; Kim, J.; O'Keeffe, M.; Yaghi, O. M. *Science* **2003**, *300*, 1127–1129.

(31) Yildirim, T.; Hartman, M. R. *Phys. Rev. Lett.* **2005**, *95*, 215504.

(32) Han, S. S.; Goddard, W. A., III. *J. Am. Chem. Soc.* **2007**, *129*, 8422–8423.

(33) Blomqvist, A.; Araujo, C. M.; Srepusharawoot, P.; Ahuja, R. *Proc. Natl. Acad. Sci. U.S.A.* **2007**, *104*, 20173–20176.

(34) Mavrandonakis, A.; Tylianakis, E.; Stubos, A. K.; Froudakis, G. E. *J. Phys. Chem. C* **2008**, *112*, 7290–7294.

(35) Han, S. S.; Goddard, W. A. *J. Phys. Chem. C* **2008**, *112*, 13431–13436.

(36) Dalach, P.; Frost, H.; Snurr, R. Q.; Ellis, D. E. *J. Phys. Chem. C* **2008**, *112*, 9278–9284.

(37) Yildirim, T.; Iniguez, J.; Ciraci, S. *Phys. Rev. B* **2005**, *72*, 153403.

(38) Dag, S.; Ozturk, Y.; Ciraci, S.; Yildirim, T. *Phys. Rev. B* **2005**, *72*, 155404.

(39) Zhao, Y. F.; Kim, Y. H.; Dillon, A. C.; Heben, M. J.; Zhang, S. B. *Phys. Rev. Lett.* **2005**, *94*, 155504.

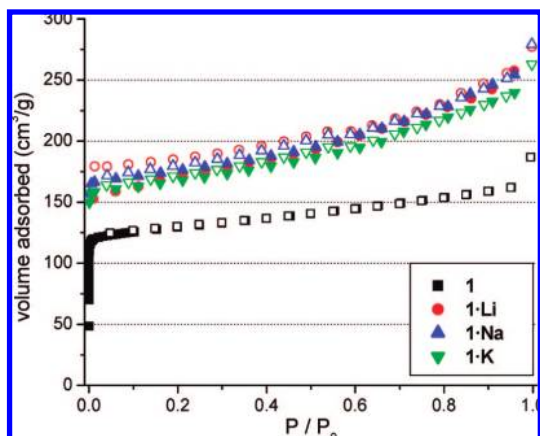


Figure 5. N₂ adsorption isotherms of **1** and **1·M**.

Recent computational work by Walton and Snurr⁴⁰ has shown, somewhat surprisingly, that BET (Brunauer, Emmett, and Teller)⁴¹ surface areas for microporous MOFs correspond closely to true surface areas, at least for N₂ as a probe molecule. As shown in Table 2, the BET surface areas for the various **1·M** materials significantly exceed those for the undoped parent material. Furthermore, the ordering of surface areas (**1** < **1·Li** < **1·K** < **1·Na**) matches the ordering for hydrogen adsorption. (Isotherms were also subjected to t-plot analyses.⁴² These analyses may be more appropriate in cases where low-pressure data are difficult to obtain. The alternative analyses return somewhat smaller micropore surface areas (ca. 20% less) and slightly different order (**1** < **1·K** < **1·Li** < **1·Na**); see Table 2. Lower surface areas are expected because, ideally at least, the t-plot analysis partitions BET-like surface areas into micropore and external (e.g., mesopore) components. We thank a reviewer for pointing out this alternative approach; additional data are included as Supporting Information.)

Another parameter of interest for hydrogen storage in MOFs, especially at high pressure, is the micropore volume.⁴³ Unfortunately, we were unable to obtain satisfactory nitrogen adsorption data for the **1·M** samples at the very low adsorbate loading required for the determination of micropore volumes via the BET approach.^{44,45} Estimates were obtainable, however, via t-plot analyses, and these are included in Table 2. Although the variations

in micropore volume for the parent versus framework-reduced materials are small, they again track the variations in hydrogen uptake. Notably, the micropore volume for **1·Li*** is about half that of **1**, as is the H₂ uptake at 1 atm.

4. Conclusions

Partial framework reduction and doping of a triply interwoven MOF with lithium, sodium, or potassium cations enhance the cryogenic uptake of H₂ by between 30 and 43% at 1 atm. The increases correspond to the uptake of as many as 13 hydrogen molecules per added cation. Remarkably, the enhancements are obtained without significant changes in heats of adsorption, implying that H₂ molecules do not interact directly with dopant metal ions. NMR measurements rule out cation solvation as an explanation for the lack of direct binding of H₂ by dopant ions. We conclude instead that the added cations are shielded by the catenated frameworks themselves from direct interaction with adsorbents. Nitrogen isotherms suggest that the key role of dopant cations and/or partial framework reduction in improving hydrogen uptake instead is to enhance the microporous surface area, presumably by facilitating the displacement of interwoven networks. Doping at higher levels, however, diminishes hydrogen uptake and reduces the N₂-accessible surface area, perhaps by blocking pore openings.

Recent computational studies suggest that MOF binding of H₂ can be increased by as much as 500% at ambient temperature and high pressure and that heats of adsorption can be increased by several kJ/mol,^{32,33} provided that direct interaction of dopant ions with hydrogen can be achieved. In efforts toward direct dopant–H₂ interaction, current work is focused on reducing and characterizing permanently microporous MOF materials comprising single rather than multiple (i.e., catenated) networks.

Acknowledgment. We thank the Office of Science, U.S. Department of Energy (grants DE-FG02-01ER15244 and DE-FG02-99ER14999) for partial support of our work. K.L.M. gratefully acknowledges a Laboratory-Grad Fellowship from Argonne National Laboratory.

Supporting Information Available: Single-crystal data for **1**, PXRD and TGA for **1**, EPR spectra for **1** and **1·Li**, complete N₂ BET, DR, and t-plot analyses of **1**, 87 K H₂ adsorption isotherms, details of isosteric heat of adsorption fitting and calculations, adsorption data for **1·Li***, and ¹H NMR spectra of evacuated and dissolved **1·M** materials. This material is available free of charge via the Internet at <http://pubs.acs.org>.

LA803014K

(45) Attempts to evaluate surface areas and micropore volumes via Ar adsorption at 87 K were similarly complicated by unacceptably slow equilibration at low gas pressures.

(40) Walton, K. S.; Snurr, R. Q. *J. Am. Chem. Soc.* **2007**, *129*, 8552–8556.

(41) Brunauer, S.; Emmett, P. H.; Teller, E. *J. Am. Chem. Soc.* **1938**, *60*, 309–319.

(42) de Boer, J. H.; Linsen, B. G.; van der Plas, T.; Zondervan, G. J. *J. Catal.* **1965**, *4*, 649–653.

(43) Frost, H.; Snurr, R. Q. *J. Phys. Chem. C* **2007**, *111*, 18794–18803.

(44) Dubinin, M. M.; Stoeckli, H. F. *J. Colloid Interface Sci.* **1980**, *75*, 34–42.